Article:
Saesin, P., Rujichit, K., Poggio, D. et al. (2026) Bioenergy production from invasive plants in the Lower Mekong Basin using hydrothermal liquefaction and anaerobic digestion. Energy Conversion and Management: X, 29. 101554. ISSN: 2590-1745

https://doi.org/10.1016/j.ecmx.2026.101554

Energy Conversion and Management: X 29 (2026) 101554

Contents lists available at ScienceDirect

Energy Conversion and Management: X

journal homepage: www.sciencedirect.com/journal/energy-conversion-and-management-x

Bioenergy production from invasive plants in the Lower Mekong Basin using hydrothermal liquefaction and anaerobic digestion

Pimnara Saesin [a], Koraporn Rujichit [a], Davide Poggio [b], William Nimmo [c], Piangjai Peerakiatkhajohn [a], Kamonwat Nakason [d], Bunyarit Panyapinyopol [d], Komgrit Wongpakam [e], Jakkapon Phanthuwongpakdee [a,*]

[a] Faculty of Environment and Resource Studies, Mahidol University, Nakhon Pathom 73170, Thailand
[b] School of Chemical, Materials and Biological Engineering, Faculty of Engineering, University of Sheffield, Sheffield S10 2TN, United Kingdom
[c] School of Mechanical, Civil and Aerospace Engineering, Faculty of Engineering, University of Sheffield, Sheffield S10 2TN, United Kingdom
[d] Department of Sanitary Engineering, Faculty of Public Health, Mahidol University, Bangkok 10400, Thailand
[e] Walai Rukhavej Botanical Research Institute, Mahasarakham University, Maha Sarakham 44150, Thailand

A B S T R A C T

Invasive plants in the Lower Mekong Basin, although ecologically challenging, offer significant potential for bioenergy. This study assessed mimosa (*Mimosa pigra*), giant salvinia (*Salvinia molesta*), and water lettuce (*Pistia stratiotes*), collected from Nakhon Phanom province, Thailand, as feedstocks for hydrothermal liquefaction (HTL) and anaerobic digestion (AD). The biomass underwent HTL treatment at 160–200 °C and was subsequently evaluated for biomethane potential (BMP). The HTL of mimosa at 200 °C for 3 h (M-200-3) yielded 16.2 wt% bio-oil (BO) and 6.98 wt% hydrochar (HC). The BO from M-200-3 possessed a higher heating value (HHV) of 31.4 MJ/kg and energy recovery efficiency (ERE) of 26.6%. Giant salvinia BO also performed effectively, with an HHV of 26.7 MJ/kg and an ERE of 23.2% at 4 h. In contrast, water lettuce showed limited HTL effectiveness, with BO yields below 10 wt%. Characterization through GC–MS revealed that phenolic compounds dominated the BO composition, while FTIR confirmed the presence of ketones, aldehydes, carboxylic acids, and aromatic rings. TGA analysis demonstrated that BO thermal degradation occurred between 261 and 314 °C, with low-boiling-point components enhancing BO performance. Additionally, SEM images revealed the formation of carbon spheres in HC at 200 °C. Energy production calculations indicated mimosa could generate 49,418 kWh of BO and 19,273 kWh of HC per hectare of feedstock (kWh/ha) under maximum annual biomass conditions. BO and HC from giant salvinia could produce 5,023 and 986 kWh/ha, respectively. Notably, water lettuce excelled in anaerobic digestion, achieving the highest BMP of 0.238 ± 0.022 NL CH_4/gVS and yielding 5,517 kWh/ha. These findings establish that invasive plant species can serve as viable bioenergy feedstocks, with mimosa optimal for HTL processing and water lettuce demonstrating superior performance in biogas production.

1. Introduction

Due to increasing energy demand, biofuels have been viewed as an alternative to unsustainable and non-renewable fossil fuels. However, employing important edible plants like corn, soybeans, and palm for biofuel has raised significant concerns about food security [1]. Consequently, there has been a shift toward utilizing non-food biomass sources, including algae, sewage sludge, and other lignocellulosic biomass, as more sustainable feedstocks for biofuel precursors.

Like in many regions, the problem of invasive plants in the Lower Mekong Basin remains unsolved. The Lower Mekong Basin includes Cambodia, Lao PDR, Thailand, and Vietnam, encompassing their water bodies and river systems that connect to the Mekong River before it flows through Vietnam and empties into the sea. Mimosa (*Mimosa pigra*), an invasive woody weed that has spread rapidly throughout the Mekong River Basin since 1970, covers about 30% of agricultural land near Kratie, Cambodia [2]. Similarly, Water lettuce (*Pistia stratiotes*) and giant salvinia (*Salvinia molesta*) are classified as pest water plant species by the Mekong River Commission [3]. In recent years, the local communities in provinces of Thailand have reported increasing difficulty with transportation and water access due to the dense growth of these invasive species [4,5]. Although efforts have been made to turn these plants into livestock feeds and organic fertilizers, their fast-growing nature continues to pose significant environmental and logistical problems [6,7]. Accordingly, scalable approaches must be developed to simultaneously mitigate the spread of these invasive species and derive value from their biomass for energy production.

Thermochemical conversion technologies, particularly hydrothermal treatment, offer a promising pathway for transforming invasive plant biomass into energy-rich products. Hydrothermal treatment

* Corresponding author.
E-mail address: jakkapon.pha@mahidol.ac.th (J. Phanthuwongpakdee).

https://doi.org/10.1016/j.ecmx.2026.101554
Received 31 July 2025; Received in revised form 30 November 2025; Accepted 12 January 2026
Available online 13 January 2026

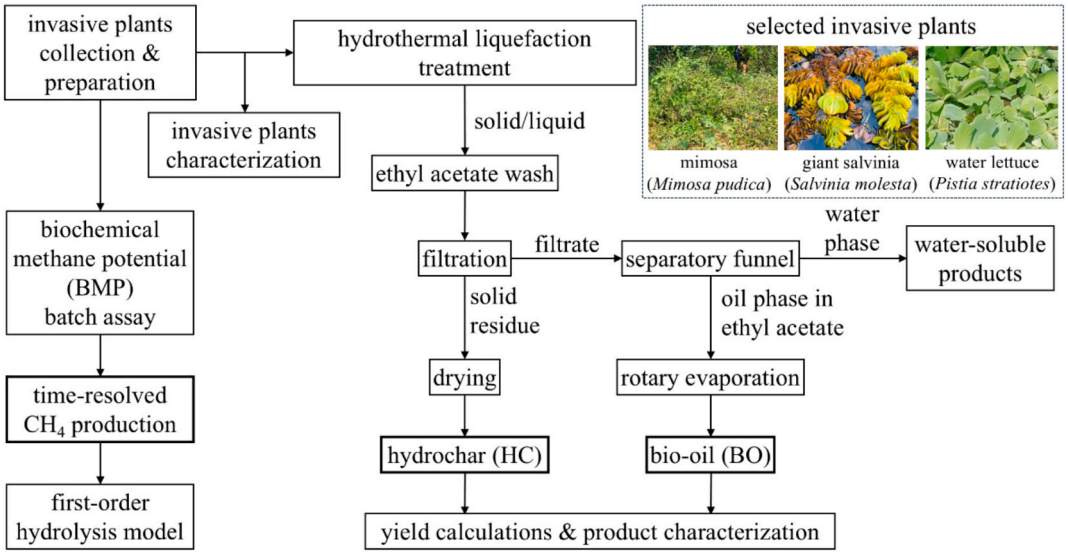

Fig. 1. Overall methodology of this study, divided into two main components: hydrothermal liquefaction (HTL) treatment and biochemical methane potential (BMP).

involves heating wet biomass or organic waste under elevated pressure and temperature to produce an energy carrier, mimicking the natural geological processes over millions of years. Hydrothermal processing offers several advantages over other thermochemical methods. The parameters and conditions can be adjusted to yield different products, such as hydrochar (HC), bio-oil (BO), and biogas. Hydrothermal liquefaction (HTL), also known as hydrous pyrolysis, converts wet biomass and other macromolecules into crude oil under moderate temperatures and high pressure through a thermochemical depolymerization process. While conventional pyrolysis requires high temperatures (400–800 °C) to convert biomass into biofuel, HTL operates at a lower temperature range (250–374 °C) and higher pressure (2–25 MPa), effectively eliminating the time and energy required for drying [8–10]. Under optimized conditions, the operating temperature for HTL can be reduced to 200 °C, as demonstrated in previous studies that converted *chlorella* into BO [11].

The trend for HTL has been increasing throughout the years, especially for microalgae, lignocellulosic biomass, and sewage sludge [12]. This growing interest in HTL aligns with the green energy transition, and the use of diverse biomass sources underscores the potential to develop a circular economy [13]. For instance, red pine sawdust processed at 350 °C yielded HC of 47% with a high heating value (HHV) of 29.3 MJ/kg [14]. In another study, coconut coir and coconut pith demonstrated an energy recovery efficiency (ERE) of 43.4% [15]. Although energy parameters were not provided in all cases, water hyacinth, an invasive aquatic plant, was successfully processed via HTL at 280 °C, yielding 8.86 wt% light oil and 26.4 wt% heavy oil. While HTL has not previously applied to giant salvinia, hydrothermal carbonization of this invasive species resulted in a 54.5 wt% HC yield with a high heating value (HHV) of 23.5 MJ/kg [16].

Anaerobic digestion (AD) is another potential technology for the valorization of invasive plant biomass. This biological process utilizes microbial activity under anaerobic conditions to convert organic matter into biogas, mainly methane (CH_4), and it is well suited for the valorization of high-moisture aquatic biomass. The biochemical methane potential (BMP) test is fundamental for evaluating CH_4 production, which depends on the organic composition of the feedstock. There is considerable previous research on a variety of freshwater macrophytes for biogas production, showing high variability of the results depending on the habitat of the plant and its age, pre-treatment and AD process conditions [17]. Studies have also examined the feasibility of community energy provision from the AD of invasive plants. For instance, in India, water hyacinth has been explored for biogas production through AD [18–20]. A village microgrid study predicted that, at optimized conditions, the energy produced by anaerobic digestion of water hyacinth could contribute to 61% of 22 MWh/year in a rural village in India, the potential biogas obtainable from the AD of water hyacinth would generate 87.6 kW and provide electricity to 934 households [20]. The integration of hydrothermal treatment and AD offers a sustainable approach for maximizing energy recovery. AD can treat hydrothermal process water containing soluble organic compounds, enabling CH_4 recovery and COD removal [21]. For example, AD achieved 61% COD removal and recovered 213 mL CH_4/gCOD from water-hyacinth-based HC process water [22].

This research aimed to investigate HTL and AD as viable technologies for managing invasive plant species in the Lower Mekong Basin while simultaneously exploring local bioenergy sources, with a primary focus on converting selected invasive plants (mimosa, giant salvinia, and water lettuce) into biofuel precursors. The study offers an innovative approach by transforming problematic invasive plants into valuable bioenergy resources, addressing two critical challenges simultaneously: environmental management and sustainable energy production through the integrated application of HTL and AD technologies.

The production of crude BO was investigated by examining the effects of different invasive plant species and various parameters on the crude BO characteristics. HC from invasive plants was also a product of HTL and was analyzed where applicable. The potential for CH_4 production from the same set of invasive plants was evaluated using BMP tests to compare the HTL pathway with the more established AD technology. The combined approach was not investigated in this study.

2. Methodology

2.1. Invasive plants collection and preparation

Mimosa, giant salvinia, and water lettuce were collected from Nakhon Phanom province, Thailand. The plants were cleaned with tap water and dried in a hot-air oven at 70 °C for at least 24 h or until constant weight was achieved. The temperature was selected to avoid changes in biomass composition prior to the HTL treatment. Dried plants were cut into small pieces and ground into powder. The powdered samples were sieved to obtain particles in the 125–500 μm size range. All samples were subjected to HTL treatment and BMP tests. The overall methodology is given in Fig. 1.

2.2. Bio-oil and hydrochar production

A standard 100 mL hydrothermal batch reactor with a Teflon chamber was used to convert invasive plants into BO and HC. The invasive plants with 125–250 μm particles (5 g) were mixed with distilled (DI) water (50 mL) in the chamber. A hot air oven was set to 150 °C before the reactor was placed inside. Then, the temperature was raised to different final setpoints of 160, 180, 200 °C, with a heating rate of 4 °C/min. Different residence times, ranging from 1 to 6 h, were tested for each temperature setpoint. Product yields were used to determine the optimal residence time. Reactions were performed under autogenous water pressure (approximately 0.62, 1.0, and 1.55 MPa at 160, 180, and 200 °C, respectively), without external gas addition. After the retention time was reached, the reactor was removed from the hot air oven and immediately quenched in running water for 30 min to stop any further reactions. The solid–liquid mixture was removed from the chamber and mixed with 250 mL of ethyl acetate to separate the water-soluble products from crude BO. The solid phase or HC was separated from the liquid phase by vacuum filtration through Whatman filter paper no.4. For the liquid phase, the ethyl-acetate-soluble product (BO) was separated from the water-soluble product using a separatory funnel. The BO was extracted from the ethyl acetate mixture using a rotary evaporator. The obtained BO and HC were dried in a hot-air oven at 80 °C for at least 24 h, until the mass was constant. The samples were stored in a desiccator cabinet for analysis.

2.3. Bio-oil and hydrochar yields calculation

The obtained BO and HC were weighed to determine the yields. Eqs. (1) and (2) calculated the yields of BO and HC (wt.%), respectively.

$$\text{BO yield (wt.\%)} = [m_{BO}\ (\text{g})/m_{dry\ biomass}\ (\text{g})] \times 100 \quad (1)$$

$$\text{HC yield (wt.\%)} = [m_{HC}\ (\text{g})/m_{dry\ biomass}\ (\text{g})] \times 100 \quad (2)$$

where $m_{dry\ biomass}$ is the oven-dried mass of the invasive plant feedstock, and masses of BO and HC are m_{BO} and m_{HC}, respectively. HHV was determined using a bomb calorimeter (Parr 6200 FE, USA), following the standard ASTM E7113. BO was used directly. HC and dry biomass samples were first pelletized using a pellet press before HHV was determined. Eq. (3) calculates the energy recovery efficiency (ERE, %), the fraction of energy from biomass retained in the product. The product yield can be either the BO or HC yield.

$$\text{ERE (\%)} = [\text{HHV of product (MJ/kg)/HHV of dry biomass (MJ/kg)}] \times \text{product yield (\%)} \quad (3)$$

2.4. Bio-oil and hydrochar characterization

The standard NREL/TP-510-42618 was used to determine lignocellulosic content. Proximate analysis was conducted in accordance with ASTM D7582-15:2015 to assess moisture, volatile matter (VM), and fixed carbon (FC). Ash content was measured following the standard analysis method, NREL/TP-510–42622. The pristine and HC samples were identified for their elemental compositions: carbon, hydrogen, nitrogen, and sulfur (CHNS) with an elemental analyzer (FlashSmart CHNS/O, Thermo Scientific, USA) with (2,5-Bis(5-*tert*-butyl-2-benzoxozol-2yl) thiophene) as a standard. Due to technical limitations, only C, H, and N were quantified for BO. The O content of each sample was calculated by deducting 100% from the C, H, N, S, and ash contents. Subsequently, C, H, and N were used to calculate the O content for BO. A scanning electron microscope (SEM, JSM-IT500LA, Japan) was used to produce surface images of HC. The surface functional groups of HC were determined by absorbance graphs produced from Fourier transform infrared spectroscopy (FTIR, Thermo Fisher Scientific, iS50, USA). The thermal stability and decomposition behavior of both BO and HC were assessed using thermogravimetric analysis (TGA) and derivative thermogravimetry (DTG) with a simultaneous thermal analyzer (Mettler Toledo, USA). Samples were placed in alumina 70 μL crucibles, and the thermal analyzer was operated at 25–900 °C (10 °C/min heating rate) under 25 mL/min N_2. Gas chromatography-mass spectrometry (GC–MS, GCMS-TQ 8040, Shimadzu, Japan) equipped with a column (SH-Rxi-5Sil MS, Shimadzu, Japan) was used to determine organic constituents in BO. Samples were diluted in ethyl acetate to 1 mg/L, and the GC–MS was set up as described in a previous study [23].

2.5. Biochemical methane potential of invasive plants

Substrates and inoculum for BMP were analyzed for total solids (TS), volatile solids (VS), total ammonia nitrogen (TAN), intermediate and partial alkalinity (IA & PA) and pH. TS and VS were determined gravimetrically following APHA standard methods: samples were dried at 105 °C for TS and combusted at 550 °C for VS [24]. pH measurements were performed using a calibrated Hach probe (Hach, USA). IA and PA were quantified by titration, using an automated titrator (Mettler Toledo, USA), to pH end points of 5.75 and 4.30, respectively [25]. TAN was measured according to the APHA method 4500-NH_3 B [24].

Batch BMP assays were conducted in 500 mL glass bottles, with triplicate samples for each substrate, inoculum blank, and positive control. Each bottle received 400 mL of inoculum sourced from a mesophilic (37 °C) lab-scale digester treating diluted pet food at an organic loading rate of 3 gVS/L/day. The inoculum was sieved (0.5 mm) and incubated in BMP bottles for 4 days to degrade residual labile organics. Before feeding the substrate, the inoculum was sampled for analysis; its characteristics were TS 2.08%, VS 1.16%, total alkalinity 8.6 g CaCO3/L, and TAN 2.2 g/L, satisfying the quality requirements suggested by a previous study [26].

Dry biomass samples were added to achieve an inoculum-to-substrate ratio (ISR) of 3 (VS basis) to minimize inhibition and ensure hydrolysis-limited CH_4 production [27]. Bottles were purged with N_2, immersed in a 37 °C water bath, and stirred at 60 rpm. Evolved gas was scrubbed of CO_2 and H_2S in 80 mL of 3 M NaOH solution, then measured by an AMPTS II system (Bioprocess Control, Lund, Sweden) with 10 mL resolution. Tests ran until daily CH_4 production <1% of the cumulative volume for three consecutive days. The performance of the inoculum was validated using cellulose controls, which resulted in a BMP of 0.376 NL CH_4/gVS ± 0.015, confirming inoculum activity [26].

Time-resolved CH_4 production data were exported from AMPTS II and were subsequently processed with custom MATLAB R2024a scripts. CH_4 volumes were corrected to STP (0 °C, 1 bar), accounting for scrubber efficiency (98% %, assumed based on manufacturer validation data for a scrubber operated at biogas production rates <3 L/day; Bioprocess Control AB, Lund, Sweden, personal communication, 2024), water vapor and initial N_2 headspace, as detailed by a previous study [28]. The data were then interpolated to a daily resolution using piecewise cubic Hermite splines and averaged across replicates. Standard deviations were propagated by quadratic addition, considering also the blank subtraction [26]. Net cumulative CH_4 production curves were normalized by VS dose to obtain the specific methane yield (SMY), expressed in NL CH_4/gVS and plotted with ±1 SD error bars.

Eq. (4) shows a first-order hydrolysis model [29], which was fitted to each SMY curve using unweighted nonlinear least squares (lsqcurvefit, MATLAB R2024a). Initial guesses of the parameters were $V_p = V(t_{end})$ and $k = 0.1$/d with bounds $0 < k \leq 10$. Ninety-five-percent confidence intervals were estimated via the asymptotic Wald method (nlparci, MATLAB) from the Jacobian and residual variance. Goodness-of-fit statistics for the model were calculated as the coefficient of determination (R^2) and the root-mean-square error (RMSE).

Table 1
Lignocellulosic content, proximate analysis, and HHV for selected invasive plants.

Sample	lignocellulosic contents (wt.%, dry basis)				proximate analysis (wt.%, dry basis)				HHV (MJ/kg)
	Cellulose	Hemicellulose	Lignin	Extractives	Moisture	Ash	VM	FC	
mimosa	21.2	17.9	31.9	22.2	8.53	5.80	65.4	20.3	19.2
giant salvinia	23.2	18.5	27.6	19.9	9.98	20.8	53.9	15.4	15.6
water lettuce	26.7	16.7	10.9	19.4	10.1	12.2	64.9	12.7	11.1

VM – volatile matter.
FC – fixed carbon

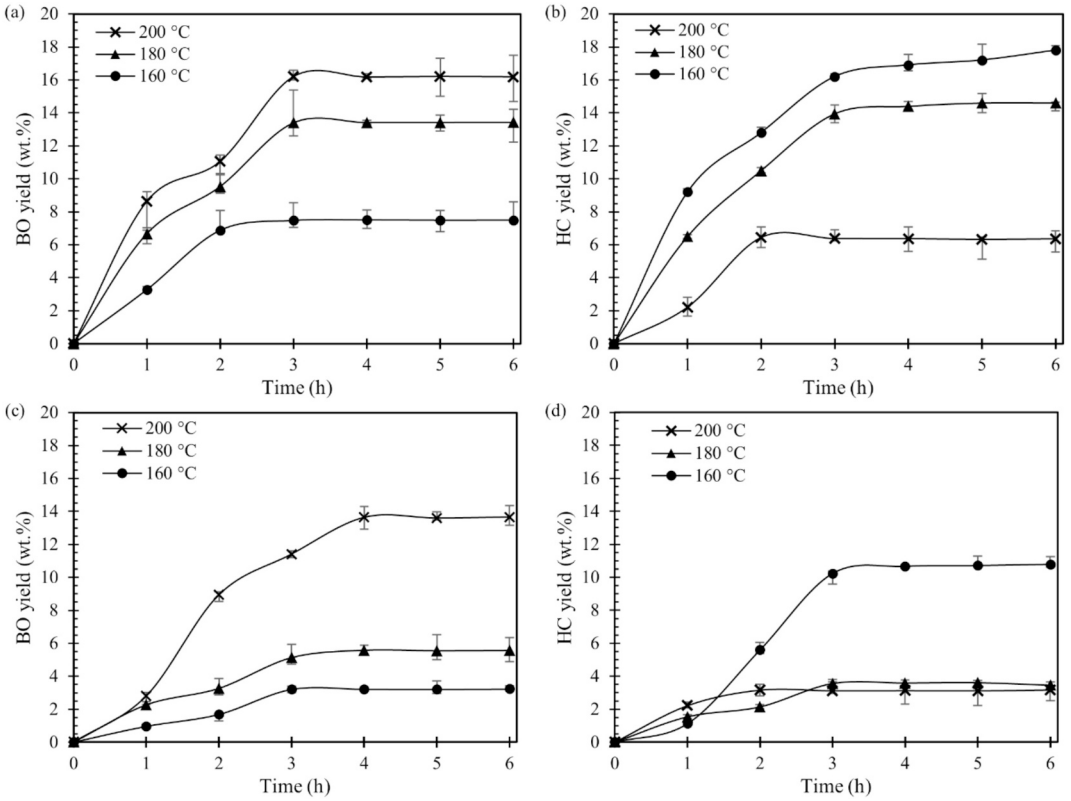

Fig. 2. Yields (wt.%) of BO and HC from mimosa and giant salvinia after 1 – 6 h of hydrothermal treatment at 160, 180, and 200 °C conditions. (a) BO yields from mimosa; (b) HC yields from mimosa; (c) BO yields from giant salvinia; (d) HC yields from giant salvinia. Eqs. 1 and 2 were used to calculate the yields.

$$V(t) = V_p(1 - \exp(-kt)) \quad (4)$$

3. Results and discussion

3.1. Invasive plants characteristics

The characteristics of prepared pristine biomass samples, including lignocellulosic composition, proximate analysis, and HHV, are summarized in Table 1. Lignocellulosic content, proximate analysis, and HHV for selected invasive plants. Among the three invasive plant species studied, Mimosa exhibited the most favorable energy profile, with a low ash content (5.80%), high lignin content (31.9%), and high extractives, which contributed to the highest HHV of 19.2 MJ/kg on a dry basis. On the other hand, water lettuce had the lowest lignin content (10.9%) and moderate ash content (12.2%), resulting in the lowest HHV of 11.1 MJ/kg among the three biomass types. Giant salvinia yielded a moderate HHV (15.6 MJ/kg). Despite its relatively high lignin content (27.6%), the biomass contained high ash content (20.8%), which limited its fuel quality. A previous study reported a much lower lignin content in giant salvinia of 12.8–14.2% [30]. Still, this variation may be due to differences in quantification methods and the geographic locations where the samples were collected. Compared to previous studies, the HHV of mimosa is comparable to that of seed oil residues, such as canola and camelina meal, which have values of 19.6 and 19.0 MJ/kg, respectively [31]. Meanwhile, the HHV of giant salvinia is similar to that of corn stalk, spirulina powder, and oat hull at 15.0, 15.4, and 15.2 MJ/kg, respectively [32,33]. These results suggest that invasive plant species, particularly mimosa, had greater energy potential than conventional biomass feedstocks.

3.2. Product yields and energy

Product yield is a key indicator for evaluating the feasibility of converting invasive plant species into bioenergy via HTL. The yields of BO and HC were calculated, and the results are shown in Fig. 2. Generally, higher reaction temperatures yielded higher BO and HC. Under subcritical water conditions, lignocellulosic biomass is widely recognized to undergo conversion into BO through a series of complex reactions, such as hydrolysis, isomerization, fragmentation, depolymerization, and condensation processes [34]. Raising the process temperature enhances the ionic product of water, making subcritical water an effective medium for facilitating both acid- and base-catalyzed

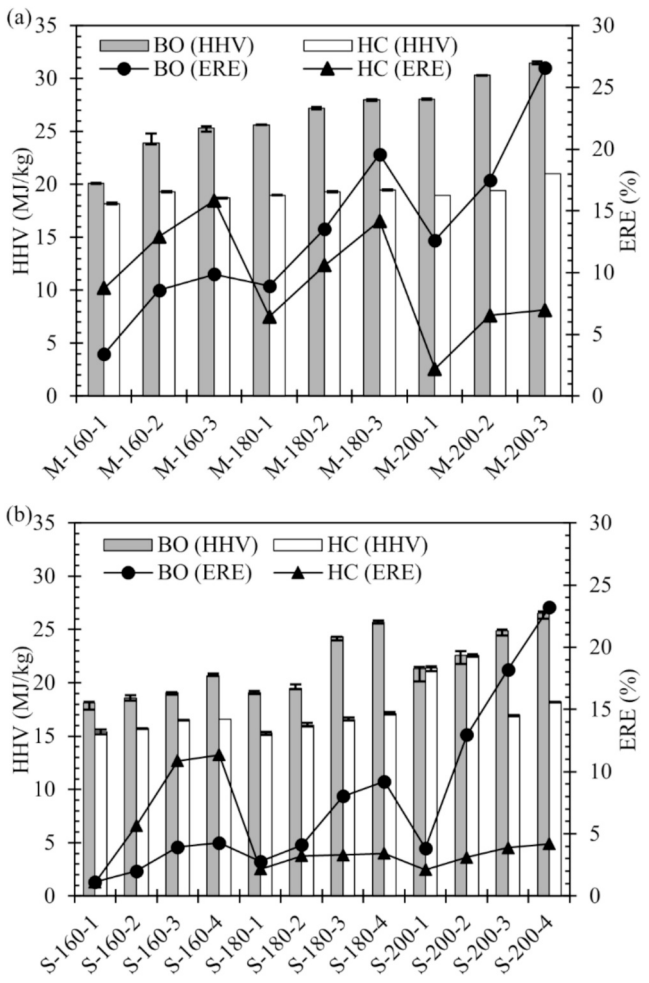

Fig. 3. HHV (MJ/kg) and ERE (%) of BO and HC at 160, 180, and 200 °C and various time conditions. (a) HHV and ERE of BO and HC derived from mimosa at 1–3 h; (b) HHV and ERE of BO and HC derived from giant salvinia at 1–4 h.

reactions [35]. HC yields exhibited an inverse trend. Increased temperature enhanced solid decomposition into BO. For mimosa, the maximum BO yield (16.2 wt%) was achieved at 200 °C, whereas the maximum HC yield (17.8 wt%) was achieved at 160 °C. For giant salvinia, optimal BO (13.7 wt%) and HC (10.8 wt%) yields were obtained at 200 °C and 160 °C, respectively. The optimum time was determined as the point at which the product yield began to level off. For mimosa, it took 3 h, whereas the yield from giant salvinia stabilized after 4 h. As a result, these values were used as the optimum hydrothermal treatment times for each invasive plant biomass. In contrast, water lettuce produced BO and HC yields of less than 10 wt% each (see Supplementary Material, Fig. S2). These minimal yields made the products difficult to handle in the experiment. Therefore, water lettuce was discontinued from further hydrothermal experiments or characterizations.

The HTL conditions selected in this study appeared to promote the conversion of mimosa into BO. According to a previous study, the amount of BO increases with increasing lignin content and decreases with increasing cellulose and hemicellulose content in the biomass [36]. Water lettuce contains the highest cellulose (~27%) and the lowest lignin (~11%) of the three weeds, whereas giant salvinia and mimosa have markedly higher lignin fractions. This might be why water lettuce produces low BO. Lignin may also take longer than cellulose and hemicellulose to form phenolic compounds [36]. Nevertheless, an HTL treatment time of more than 1 h would be sufficient to convert lignin-rich biomass into crude BO [36]. Furthermore, operating at 200 °C appeared to enhance hydrolysis and dehydration reactions compared to lower temperatures at 180 and 160 °C, thereby increasing the yield of BO.

Sample identifiers are used for BO and HC products to clarify the results under various experimental conditions. Each identifier indicates the invasive species, the treatment temperature, and the treatment duration. For instance, M-160-1 represents a product derived from mimosa that has been subjected to hydrothermal treatment at 160 °C for 1 h. In comparison, S-200-4 represents a product derived from giant salvinia that has been subjected to hydrothermal treatment at 200 °C for 4 h.

ERE represents the proportion of the original feedstock's energy retained in the product following HTL, while the HHV indicates the energy content of the resulting fuel [37]. HHV and ERE are presented in Fig. 3, with corresponding numerical data provided in the Supplementary Material (Table S2 and Table S3). Generally, BO exhibited superior HHV compared to HC. The BO of M-200-3 had the highest HHV and ERE, at 31.4 MJ/kg and 26.6%, respectively. For S-200-4, its BO possessed the HHV and ERE of 26.7 MJ/kg and 23.2%, respectively. These HHV results were comparable to a recent study on BO derived from crude olive pomace, which had an HHV of 32 MJ/kg [38]. However, the ERE of crude olive pomace was exceptionally high at approximately 60% [38]. The BO derived from cassava rhizome showed a similar HHV of 23.1 MJ/kg and a comparable ERE of 37.5% [39]. Among HC products, the highest ERE was from M-160-3 at 17.8%, with a corresponding HHV of 21.0 MJ/kg. Based on HHV values and ERE, mimosa appears to be a more promising precursor than giant salvinia. This may be because mimosa has lower ash content and higher lignin and extractives compared to giant salvinia. The compositional and thermal characteristics of BO and HC could further explain this phenomenon.

3.3. Bio-oil and hydrochar properties

The elemental composition of HTL products is shown in Fig. 4. Compared to pristine biomass, BO exhibited significantly higher carbon (C) content, which further increased with rising HTL temperatures. Conversely, the oxygen (O) content in BO was substantially lower than that in raw biomass and decreased with increasing temperature. Retention time, however, had only a minimal effect on both C and O levels. These shifts indicated deoxygenation reactions during the process [40]. As a result, the higher carbon and lower O contents contributed to a significantly elevated HHV of BO relative to raw biomass, with HHV improving as the processing temperature increased. Among all the products, M-200-3 possessed the highest C content for both BO and HC, consistent with its superior product yields and energy results. High lignin biomass yields BO with higher HHV and ERE because of the low H/C ratio typical of lignin and the dominance of heavy organics in the resulting BO [41]. The H/C and O/C ratios of HTL-derived BO, for both mimosa and giant salvinia, become increasingly similar to those of diesel with rising temperature, as demonstrated by their proximity on the Van Krevelen diagram (Fig. 4c). For the HC products (Fig. 4d), S-200-4 started to enter the peat zone as the O/C ratio decreased with increasing temperature conditions. On the other hand, M-160-3 was located at the intersection of peat and lignite. The HC products of mimosa shifted toward higher H/C ratios due to decarboxylation. Except for salvinia-derived HC products, all other products displayed an early heating stage where dehydration was the primary influence, transitioning to dominance by decarboxylation in later stages. A similar phenomenon was shown in the HTL of microalgae and sewage sludge [42,43].

GC–MS detected volatile and semi-volatile BO components. The non-volatile compounds remain uncharacterized. Fig. 5 shows the relative abundance (% of total GC-MS peak area) of compound classes in BO samples, determined from peak area integration of GC–MS chromatograms. The actual areas under the GC–MS chromatograms for the compounds are provided in the Supplementary Material (Table S4). In Mimosa-derived BO, ester was the dominant compound class present in M-160-3, whereas phenolic compounds became the dominant class in M-

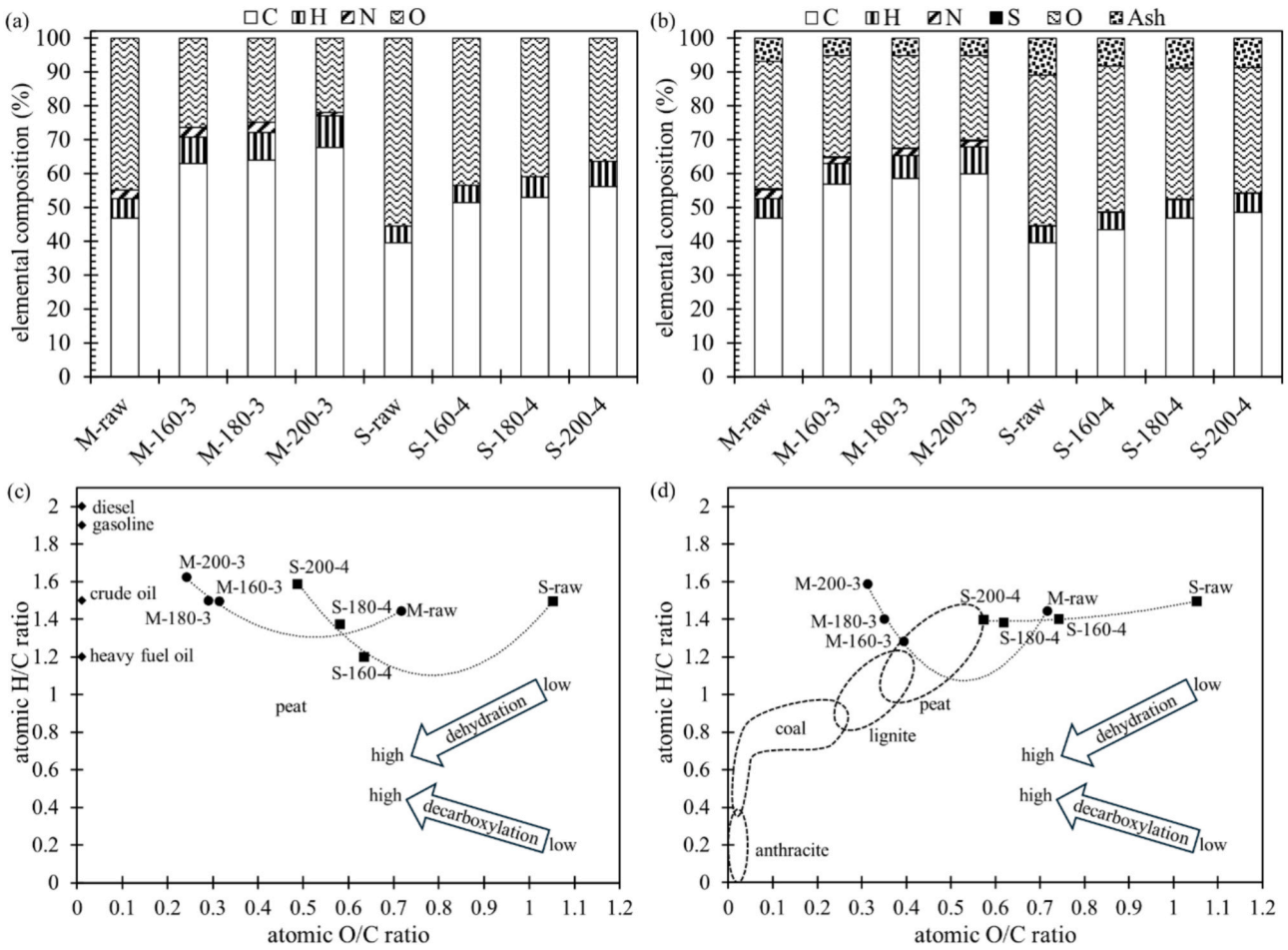

Fig. 4. Elemental composition (%) of BO and HC after hydrothermal treatment at 160, 180, and 200 °C and optimum time conditions. (a) BO of mimosa at 3 h and salvinia at 4 h; (b) HC of mimosa at 3 h and giant salvinia at 4 h; (c) Van Krevelen diagram for BO in comparison to conventional fuel oil; (d) Van Krevelen diagram for HC in comparison to conventional solid fuels.

180-3 and M-200-3. This coincided with the elemental trends shown in Van Krevelen diagram (Fig. 4c). In the early stage, light esters such as propanoic acid and formic acid would form from residual carbohydrates or extractives. For Giant salvinia-derived BO, the volatile fraction at 180–200 °C, acids were decarboxylated, and lignin degradation and depolymerization took place more often with mimosa products to create phenolic species like 1,2,3-Benzenetriol and 2,4-Di-*tert*-butylphenol. For giant salvinia BO products, the volatile fraction at 180–200 °C was mainly composed of phenolic compounds, especially catechol, which was probably derived from carbohydrate fragmentation and lignin. The presence of phenolic compounds contributes to the aromatic richness and potential calorific value of the BO. At the same time, hydrocarbon-like compounds such as campesterol, stigmasterol, gamma-sitosterol, and isophytol decreased, likely due to their thermal instability and subsequent degradation at these temperatures.

The FTIR results are displayed in Fig. 6 and Supplementary Material (Table S5–S6). All samples exhibited the broad O-H stretch around 3200–3400 cm^{-1}. Both pristine samples of mimosa and giant salvinia exhibited C-H stretching bands around 2905 and 2858 cm^{-1}, corresponding to the presence of the CH_2 and CH_3 functional groups typically found in lignocellulosic contents [44]. These functional groups were still present in BO and HC. A shoulder band at approximately 1720–1730 cm^{-1} was detected only in the biomass samples and can be assigned to carboxyl or carbonyl functional groups associated with lignin structures [45]. All BO samples exhibited a distinct C═O stretching around 1700 cm^{-1}, corresponding to the presence of mono-alkyl ester, ketones, aldehydes, and carboxylic acids [46]. The same peak was observed, though less prominently, in HC samples. The peaks at approximately 1600–1610, attributed to aromatic ring vibrations, were observed in all samples [45]. Absorption bands at 1500–1510 cm^{-1}, attributed to aromatic C═C stretching vibrations, were observed in both BO and, to a lesser extent, HC, suggesting the presence of phenolic compounds [47]. C–N stretching vibrations were observed at approximately 1370–1470 cm^{-1} in all samples, with some variation in intensity. A prominent peak around 1035 cm^{-1} of biomass corresponded to the C-O-C pyranose ring skeletal vibration in cellulose [48]. This peak was also detected in the HC samples, though with diminished prominence. Additionally, the C-O stretching bands of BO, at approximately 1045 and 1005 cm^{-1}, corresponded to those of phenol and esters [46]. These FTIR-detected functional groups were consistent with the molecular compounds identified by GC–MS (Fig. 5).

SEM images of HC are also shown in Fig. 6. The surfaces of raw mimosa and salvinia exhibited smooth, layered surface textures. At 160 °C, the derived HC exhibited intermediate changes, with some roughness while retaining some of its original smoothness. The HC of S-180-4 had an irregular surface appearance, whereas M-180-3 began forming carbon spheres. At 200 °C, well-defined carbon spheres became prominent on the surface of the HC products from both plants. The formation of these carbon spheres typically occurs through four stages: dehydration, condensation, polymerization, and aromatization, with time, temperature, and catalysts playing crucial roles [49]. The experimental conditions employed in this study successfully achieved the requirements for sphere nucleation.

The thermal characteristics of BO are illustrated by TGA and DTG

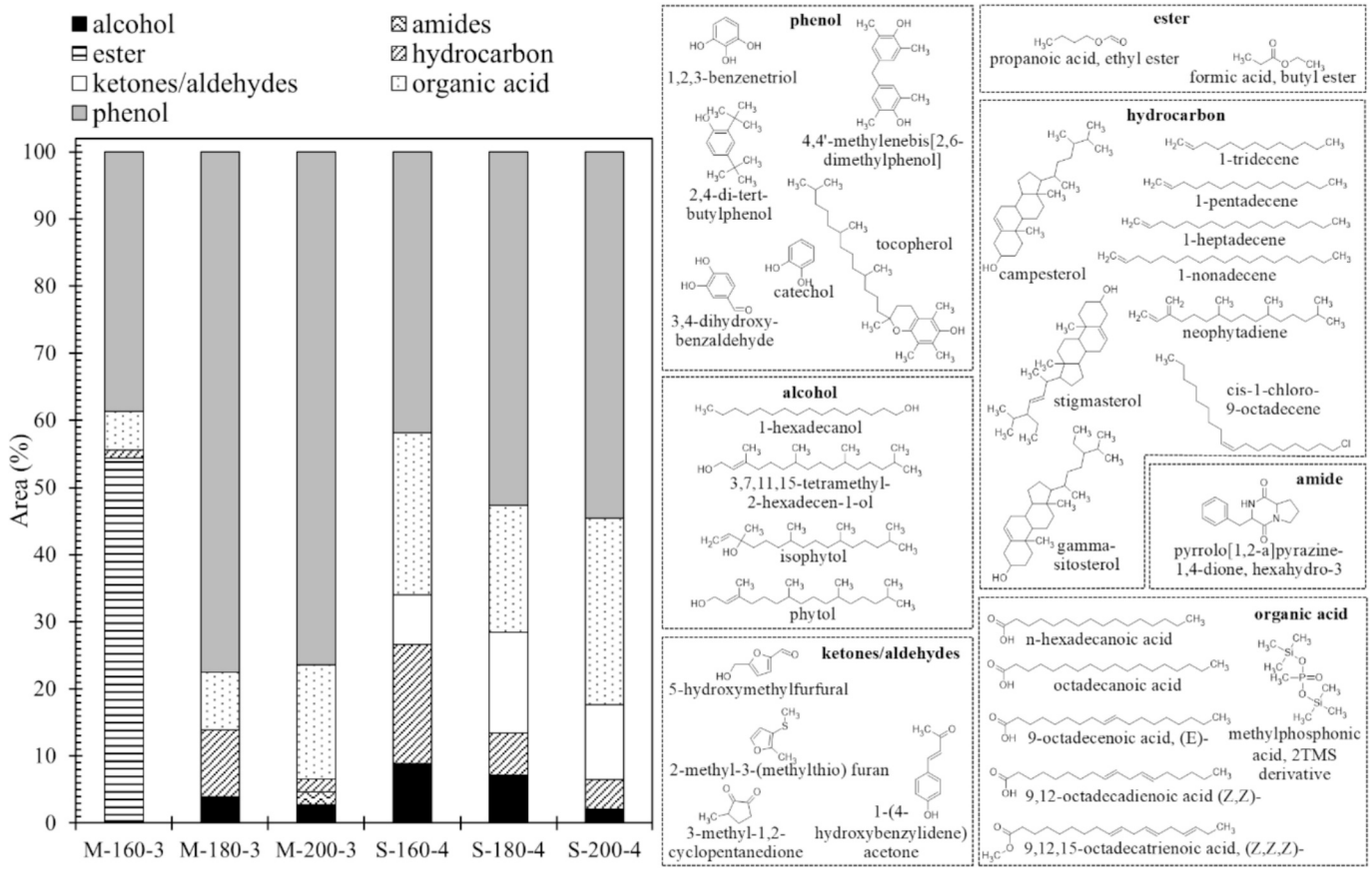

Fig. 5. GC–MS analysis of BO samples showing relative abundance of seven major compound classes (alcohols, amides, esters, hydrocarbons, ketones/aldehydes, organic acids, and phenols), with corresponding structures of molecules detected in each class.

curves, as shown in Fig. 7. Approximately 10% of the pristine samples were lost due to dehydration at temperatures ranging from 100 to 150 °C. The majority of the mass loss for each sample occurred between 150 and 500 °C, consistent with the thermal decomposition of biomass components. Raw mimosa and giant salvinia exhibited maximum temperatures (T_{max}) of 332 °C and 320.5 °C, respectively. This was typical biomass thermal behavior, as similar results have been shown in other water plants and agricultural residues [50]. In contrast, BO showed several peaks in the degradation temperature range, which may be due to the sample's complex composition. For instance, M-200-3 had a T_{max} of around 261–314 °C, indicating that the majority of the volatile content was lost within that range. However, some components in the samples may also have a T_{max} around 390 °C. Although the increase in temperature did not create a noticeable trend in TGA and DTG, the experiment revealed that HTL facilitates the formation of low-boiling components. This transformation enhances the fuel potential of BO by increasing its volatile fraction and reducing the thermal stability of its components [51].

3.4. Biochemical methane potential of invasive plants

The 42-day BMP trials confirmed a clear performance hierarchy among the invasive plants: water lettuce > giant salvinia > mimosa. Table 2 displays CH4 and energy yields of the invasive plants. Water lettuce produced 0.238 ± 0.022 NL CH_4/gVS, almost twice the CH_4 obtained from mimosa (0.119 ± 0.010 NL/gVS) and giant salvinia (0.127 ± 0.011 NL/gVS) and reached 63% of the cellulose control. Relative standard deviations were below 10%, indicating good repeatability across replicates.

The compositional profile of the substrates explains these differences. Unlike HTL, the AD process seemed to favor high-cellulose biomass like water lettuce. Because lignin is essentially non-biodegradable under anaerobic conditions, it forms a physical and chemical barrier that impedes microbial access to the otherwise fermentable cellulose and hemicellulose matrix; it also adsorbs hydrolytic enzymes, diverting them from productive action [52]. Previous extensive cross-dataset analyses showed that lignin concentration is the single strongest negative predictor of BMP across diverse feedstocks [53]. The present results reinforce this relationship and underscore the need for pretreatment, mechanical, chemical, or biological, when high-lignin biomasses, such as mimosa or giant salvinia, are targeted for biogas production [54]. ERE values indicate the low degradability of mimosa and giant salvinia, with AD recovering only 23–24% of the energy content of the substrates, compared to almost 50% for the more degradable water lettuce.

Literature BMP data for water lettuce reported a yield of 0.39 NL CH_4/gVS for the whole plant and 0.30 NL CH_4/gVS for roots only, with a 60-day duration of the batch test, an ISR of 1 (VS basis) and using digested cow manure as inoculum [55]. Another work achieved up to 0.24 NL CH_4/gVS in BMP tests conducted at different inoculum-to-substrate ratios, employing digested sludge as inoculum at a relatively low ISR (between 0.06 and 0.2) and therefore requiring longer duration of the test up to 73 days [56]. Therefore, the results of the present study align with the lower end of the literature data.

For giant salvinia, a previous study performed both BMP tests and pilot-scale batch digestions [57]. In the BMP tests, using a relatively low ISR (actual values not reported) and digested sludge plus food waste as a source of inoculum, salvinia produced only 52 ± 55 L biogas/kgVS, more than three times lower than water hyacinth and cabomba, confirming its relatively recalcitrant nature [57]. In the pilot-scale batch reactor, the study reported a biogas yield of 155 L/kgVS with an average CH_4 content of about 50%, corresponding to about 0.08 NL CH_4/gVS,

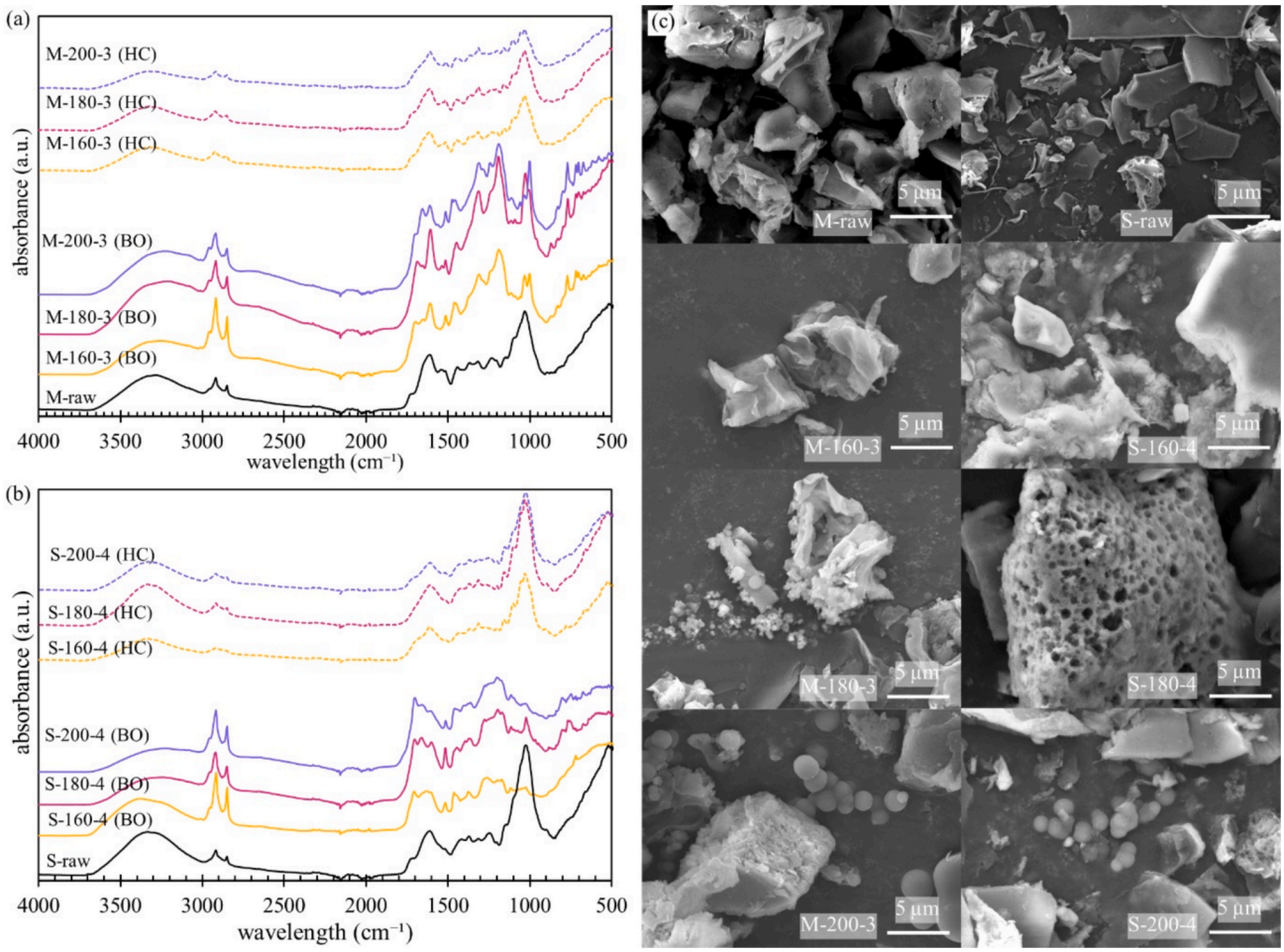

Fig. 6. Surface characteristics of BO and hydrochar HC after hydrothermal treatment at 160, 180, and 200 °C and optimum time conditions. (a) FTIR spectra of mimosa products at three h; (b) FTIR spectra of giant salvinia products at 4 h; (c) SEM images of HC.

and a k value of 0.047/day, again lower than for the other weeds (water hyacinth and cabomba) [57]. Given the different inoculum loading and reactor scales in the study, the higher yield (0.13 NL/gVS) and first-order rate (0.148/day) obtained seem to represent an upper bound for raw giant salvinia without chemical pretreatment [57].

No peer-reviewed BMP data were found for mimosa. The present study thus provides the first calibrated value for this species. The lowest CH_4 yield among the three substrates may have been influenced by the methane-suppressing effect of condensed tannins, which are documented in rumen studies, where substitution with mimosa foliage reduced CH_4 formation by 20–45% [58].

The first-order hydrolysis model fits can be found in Fig. 8, while their fitting parameters are tabulated in Table 3. The model reproduced 94–98% of the variance in the cumulative methane curves (R^2 = 0.94–0.98), with low residual errors (RMSE = 0.005–0.018 NL CH_4/gVS). The fitted plateau volume (V_p) closely matched the experimental BMP, with relative confidence intervals of ±2–2.5%, whereas the confidence intervals for the rate constant k were wider, at ±9–12%, reflecting greater uncertainty in the rate estimates.

Although mimosa had the lowest ultimate yield, it exhibited the highest k (0.202/day). Conversely, giant salvinia degraded most slowly (k = 0.149/day) and reached a plateau at the lowest methane volume. Water lettuce combined a comparatively high V_p with an intermediate k, making it the best overall performer. Its cumulative production curve displayed a mildly sigmoidal profile, characteristic of a Gompertz-type response with a short initial lag phase preceding active degradation. A three-parameter sigmoidal model, such as the modified Gompertz, would represent this lag more explicitly, but given that the first-order model already describes the data well and preserves the same ranking between substrates, it was retained here for consistency and parsimony.

When HTL co-products are considered, the process captured substantially more of the feedstock energy than AD for the woody invaders, but not for the soft-tissue species. For mimosa, summing the 26.6% retained in BO with the 17.8% locked in hydrochar, under the best process conditions, yields a total HTL ERE of 44.4%, almost double the 23.2% recovered as CH_4 in AD. Giant salvinia BO preserved 16.2% of the initial energy, and the accompanying HC contributed 17.8%, resulting in an overall HTL ERE of approximately 34%. This was only about ten percentage points higher than the 24.7% realized through AD. In sharp contrast, water lettuce achieved the opposite pattern: AD recovered 49.3% of its energy content, whereas HTL retained <10% in total, underlining that feedstock composition ultimately decides whether HTL or AD is the superior valorization route.

3.5. Estimation of energy production from invasive plants

Energy production estimates based on the sampled dry biomass of invasive plant species are presented in Table 4. While the energy estimates were calculated based on the results of this work (Sections 3.2 and 3.4), the amounts of dry biomass presented for the Lower Mekong Basin were obtained from previous studies [59–61]. Eq. S1 (Supplementary Material) was used to calculate the estimated energy. Due to limited sampling data for giant salvinia in the Lower Mekong Delta, a study conducted in Puerto Rico was utilized as a reference [62]. Moreover, it is

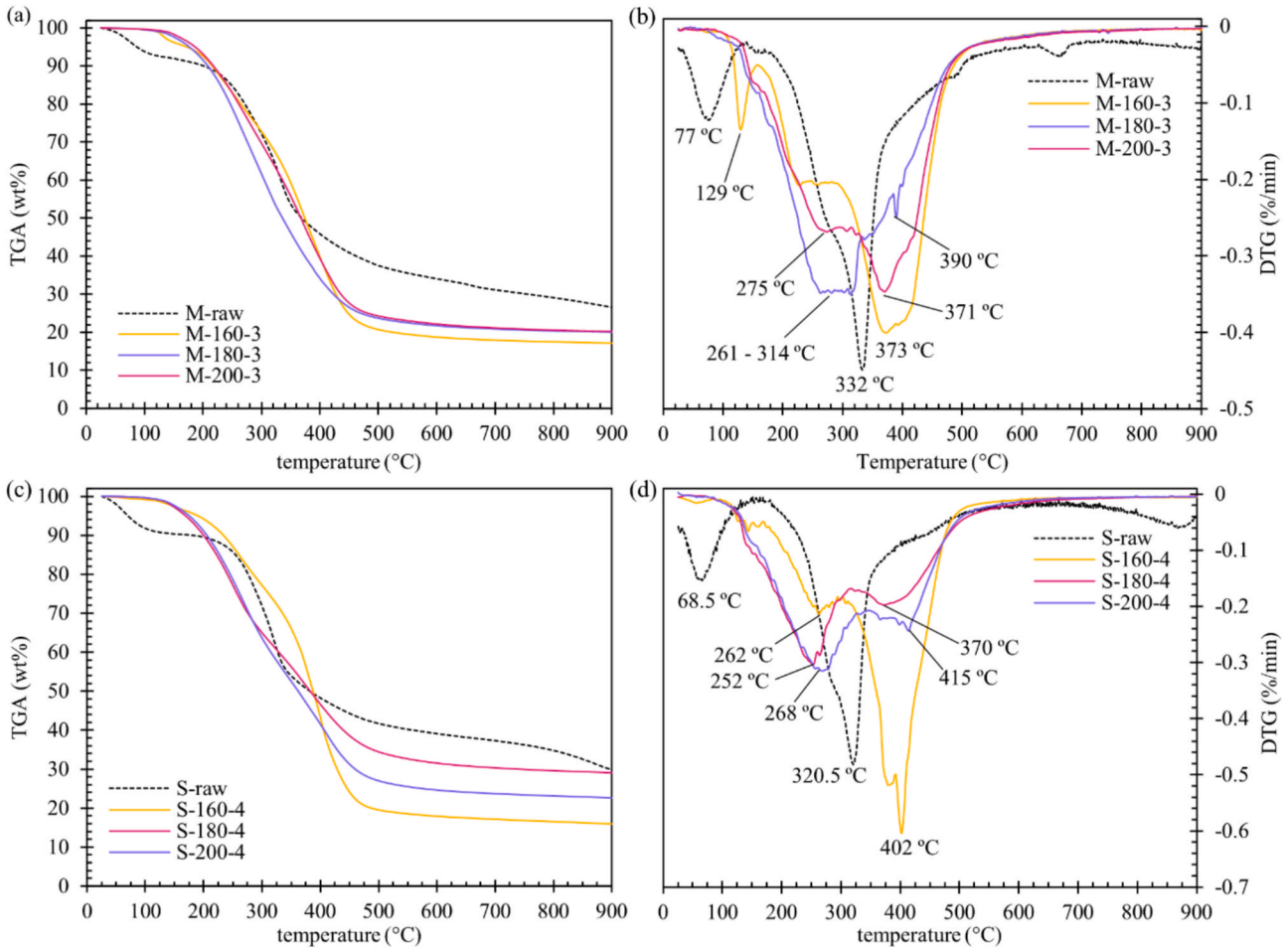

Fig. 7. Thermal characteristics of BO after hydrothermal treatment at 160, 180, and 200 °C and optimal time conditions. (a) TGA results of BO made from mimosa at 3 h; (b) DTG results of BO made from mimosa at 3 h; (c) TGA results of BO made from giant salvinia at 4 h; (d) DTG results of BO made from giant salvinia at 4 h.

Table 2
CH_4 and energy yields of the invasive plants on VS and fresh matter basis.

Substrate	CH_4 yield on VS (NL CH_4/gVS)	RSD (%)	VS content substrate, dry basis (%)	energy yield substrate, dry basis (MJ/kg) [a]	ERE (%)
cellulose (control)	0.376 ± 0.015	4.1%	100	14.96	
mimosa	0.119 ± 0.010	8.5%	94.0	4.45	23.2%
giant salvinia	0.127 ± 0.011	8.7%	76.1	3.86	24.7%
water lettuce	0.238 ± 0.022	9.1%	57.8	5.47	49.3%

a. Higher heating value (HHV) of CH_4 is 39.8 MJ/m^3.
RSD – relative standard deviation
VS – volatile solid.

important to note that the estimated energy values were overestimated due to the exclusion of suitable energy conversion efficiencies (Table 4). With a dry biomass of 679 g/m^2, BO and HC from mimosa could provide about 15,763 and 6,147 kWh/ha, respectively. The energy yielded from CH_4 produced through AD of the mimosa was calculated to be 8,402 kWh, higher than that of HC. However, when using the maximum annual results, mimosa can produce about 2.13×10^4 kg/ha. This would produce up to 49,418, 22,054, and 26,023 kWh worth of energy from BO, HC, and AD, respectively. Giant salvinia produced significantly lower dry biomass per hectare than mimosa. Energy outputs from its BO, HC, and BMP were estimated at 5,023, 986, and 3,140 kWh/ha, respectively. For water lettuce, the only available results for energy yields were from the BMP experiment. According to biomass availability from Nong Han Kumphawapi, Thailand, a hectare of water lettuce would produce approximately 5,517 kWh. Although the water lettuce achieved higher CH_4 and HHV yields on a dry-matter basis than mimosa, its biomass production was lower, resulting in lower overall energy production from CH_4.

It should be noted that while HC produced the lowest maximum energy, its production process required the fewest resources. In contrast, separating BO from the solid phase required a substantial amount of ethyl acetate (over 250 mL per 5 g of substrate) and subsequent solvent evaporation. Similarly, anaerobic digestion will require a long retention time (>40 days) to achieve maximum biogas production. Actual dry biomass per hectare in other areas of the Lower Mekong Basin may vary from the values reported in Table 4. Consequently, energy production will vary depending on growth rates and the associated dry biomass yields of the chosen invasive plants. Lastly, this study excluded transportation costs and other localized economic analyses. The need for specific energy production methods or combined systems will largely depend on the contextual requirements of the area utilizing bioenergy production.

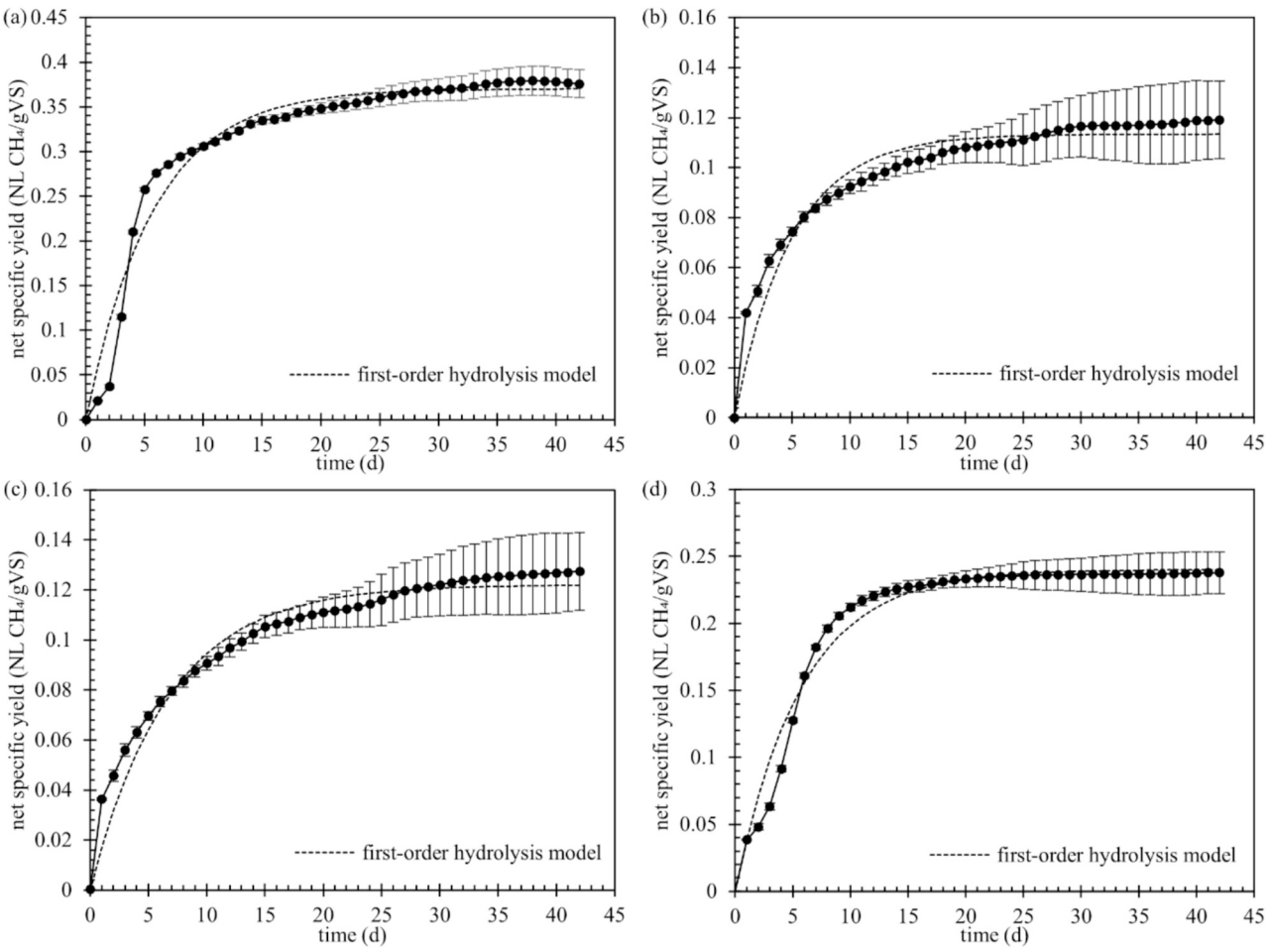

Fig. 8. Net specific yield (NL CH_4/gVS) from the BMP experiments and their respective first-order hydrolysis model. (a) cellulose (control); (b) mimosa; (c) giant salvinia; (d) water lettuce.

Table 3
Fitting parameters of the first-order hydrolysis model of invasive plants BMP with cellulose as a reference.

Substrate	V_p	Confidence interval V_p		k	Confidence interval k		R^2	RMSE
Cellulose	0.370	0.362	0.378	0.174	0.155	0.193	0.963	0.018
Mimosa	0.113	0.110	0.115	0.202	0.178	0.225	0.941	0.006
Giant salvinia	0.122	0.119	0.124	0.148	0.134	0.163	0.958	0.005
Water lettuce	0.240	0.235	0.244	0.174	0.159	0.190	0.975	0.010

V_p – ultimate methane potential (NL CH_4/gVS).
k – first order rate constant (1/day).
R^2 – coefficient of determination
RMSE – root-mean-square error.

All in all, this study demonstrated that invasive plants from the Lower Mekong Basin, including mimosa, giant salvinia, and water lettuce, demonstrated potential as viable bioenergy feedstocks. Mimosa and giant salvinia are better suited for BO and HC production via hydrothermal treatment. Despite mimosa's high biomass abundance, water lettuce exhibited higher CH_4 yield per unit mass and emerged as a promising substrate for biogas production.

Further investigations are required to advance this research. First, the solvent extraction protocol used a notably high solvent-to-biomass ratio of 50:1 (250 mL of ethyl acetate per 5 g of biomass). Future studies should systematically optimize this parameter to reduce solvent use while maintaining effective extraction efficiency, thereby enhancing the environmental sustainability and economic viability of the process. Second, the research should investigate the potential utilization of HTL process water, which may contain nutrients and organic compounds. Third, comprehensive upscaling analyses are crucial to assessing the practical applicability of this technology. Such evaluations should include energy input–output balances, techno-economic feasibility studies, and engineering considerations for pilot-scale implementation. Lastly, future work should incorporate empirical data specific to the invasive plant species under study and actual energy conversion efficiency.

4. Conclusions

This study demonstrated that invasive plant species from the Lower Mekong Basin can serve as viable bioenergy feedstocks through various conversion pathways. Mimosa showed the highest HTL conversion, producing 16.2 wt% BO and 17.8 wt% HC at 200 °C for 3 h (M-200-3). Its BO reached a HHV value of 31.4 MJ/kg and ERE of 26.6%. The

Table 4
Estimated maximum energy production per hectare of invasive plants (kWh/ha).

Invasive plants	Dry biomass (g/m^2)	Dry biomass per hectare (kg/ha)	Maximum Estimated energy per hectare of dry biomass (kWh/ha)			Reference sampling site	Ref.
			HTL – BO [a]	HTL – HC [a]	AD [b]		
Mimosa	679[c]	6.79×10^3	15,763	6,147	8,402	Tram Chim National Park, Vietnam	[59]
	n/a	5.80×10^3 [d]	13,457	5,248	7,177	Dong Thap Province, Vietnam	[60]
	n/a	2.13×10^4 [e]	49,418	19,273	26,023		
Giant salvinia	293[f]	2.93×10^3	5,023	986	3,140	Las Curias Reservoir, Puerto Rico [g]	[62]
Water lettuce	363[c]	3.63×10^3	n/a	n/a	5,517	Nong Han Kumphawapi, Thailand	[61]

n/a – not available.
a – calculated from Eq. S1 (Supplementary Material) and the samples with the highest HHV and ERE; values may be overestimated, as energy conversion efficiency was not considered.
b – calculated from Eq. S1 (Supplementary Material) and the HHV of the produced CH_4 in BMP tests; values may be overestimated as energy conversion efficiency was not considered (this.
c – temporal results.
d – minimum annual results.
e – maximum annual results.
f – temporal results calculated from a quadrat.
g – location is not from the Lower Mekong Basin

species' high lignin content promoted the formation of phenolic compounds during thermal processing, with acids decarboxylating at 180–200 °C to generate phenolic compounds, including 1,2,3-benzenetriol and 2,4-di-*tert*-butylphenol. This biochemical transformation, coupled with mimosa's abundance of 2.13×10^4 kg/ha (temporal), produced substantial energy outputs of 49,418 kWh for BO and 19,273 kWh for HC per hectare under optimal conditions. The Van Krevelen diagram analysis further indicated that increasing the HTL temperature improved the H/C and O/C ratios of the BO, making them more similar to those of diesel fuel.

Giant salvinia underwent similar hydrothermal treatment patterns, with phenolic-rich volatile fractions forming at 180–200 °C. However, its lower lignin content and biomass availability generated reduced energy yields of 5,023 kWh BO and 986 kWh HC per hectare.

Water lettuce presented a contrasting profile, producing minimal yields through hydrothermal treatment (less than 10 wt% BO and HC) but excelling in anaerobic digestion with the highest BMP of 0.238 ± 0.022 NL CH_4/gVS. This superior performance in biogas production was attributed to its elevated cellulose content and reduced lignin content. The cellulose-rich composition enabled more efficient microbial conversion compared to lignin-rich giant salvinia and mimosa, which exhibited inhibitory effects on biogas production. Due to its moderate biomass growth yield, water lettuce was estimated to produce 5,517 kWh per hectare.

The composition of the feedstock ultimately determined whether HTL or AD was the more suitable valorization pathway. In terms of production, HC required fewer resources than BO, which necessitated substantial use of ethyl acetate (>250 mL per 5 g substrate) and subsequent solvent evaporation. Furthermore, biogas production required longer processing periods to achieve maximum yields. Actual energy generation varied with species-specific growth rates, corresponding dry biomass yields, and processing resource needs.

Future research should optimize the solvent quantity, utilize the HTL process water, conduct comprehensive upscaling and techno-economic analyses, incorporate species-specific data, and determine the actual energy efficiency to enhance the practical viability of converting invasive plants in the Lower Mekong Basin into bioenergy. Overall, this study highlights that invasive species such as mimosa, giant salvinia, and water lettuce have promising potential as bioenergy feedstocks, contributing to regional energy security in the Lower Mekong Basin.

CRediT authorship contribution statement

Pimnara Saesin: Writing – original draft, Investigation, Formal analysis, Conceptualization. **Koraporn Rujichit:** Writing – original draft, Visualization, Data curation. **Davide Poggio:** Writing – review & editing, Software, Formal analysis. **William Nimmo:** Validation, Resources. **Piangjai Peerakiatkhajohn:** Writing – review & editing, Visualization, Resources. **Kamonwat Nakason:** Writing – review & editing, Methodology. **Bunyarit Panyapinyopol:** Validation. **Komgrit Wongpakam:** Resources. **Jakkapon Phanthuwongpakdee:** Writing – review & editing, Supervision, Project administration, Funding acquisition, Conceptualization.

Declaration of competing interest

The authors declare that they have no known competing financial interests or personal relationships that could have appeared to influence the work reported in this paper.

Acknowledgements

This work is supported by the Strategic Research Fund (Starter, Contract no. MU-SRF-ST-01A/67) granted by Mahidol University and by the UK ISPF Institutional Support Grant (ODA) funding scheme, granted by the University of Sheffield.

Appendix A. Supplementary data

Supplementary data to this article can be found online at https://doi.org/10.1016/j.ecmx.2026.101554.

Data availability

Data will be made available on request.

References

[1] Boly M, Sanou A. Biofuels and food security: evidence from Indonesia and Mexico. Energy Policy 2022;163. https://doi.org/10.1016/j.enpol.2022.112834.
[2] Rijal S, Cochard R. Invasion of Mimosa pigra on the cultivated Mekong River floodplains near Kratie, Cambodia: farmers' coping strategies, perceptions, and outlooks. Reg Environ Chang 2015;16:681–93. https://doi.org/10.1007/s10113-015-0776-3.
[3] Mekong River Commission. Preliminary Design Guidance for Proposed Mainstream Dams in the Lower Mekong River Basin. Vientiane: 2023.
[4] Na Ayutthaya ST, Tubmanoch S. อุดรธานีเร่งแก้ "จอกหูหนูยักษ์" ระบาดในทะเลบัวแดง. National News Bureau of Thailand 2022.
[5] Saiwaew J, Tubmanoch S. จังหวัดหนองคาย เร่งกำจัดจอกแหน ที่กระทบการทำประมงและทำให้น้ำท่วม. National News Bureau of Thailand; 2023.
[6] Laeadon K. Applying of bagasse, rice straw and giant mimosa as cultivation substrate of oyster mushroom (*Pleurotus ostreatus* Jacq.ex Fr.). J Agric Res Extension 2021;39:28–39.

[7] Benjawan L, Chaikongdee T. Co-composting of hair waste, water lettuce, pig manure and it's effect to the Amaranth (*Amaranthus hybridus L.*) growth. King Mongkut's Agric J 2019;37:498–506.

[8] Mathanker A, Das S, Pudasainee D, Khan M, Kumar A, Gupta R. A review of hydrothermal liquefaction of biomass for biofuels production with a special focus on the effect of process parameters, co-solvents, and extraction solvents. Energies (Basel) 2021;14:4916. https://doi.org/10.3390/en14164916.

[9] Prurapark R, Owjaraen K, Saengphrom B, Limthongtip I, Tongam N. Effect of temperature on pyrolysis oil using high-density polyethylene and polyethylene terephthalate sources from mobile pyrolysis plant. Front Energy Res 2020;8. https://doi.org/10.3389/fenrg.2020.541535.

[10] Elhassan M, Abdullah R, Kooh MRR, Chou Chau Y-F. Hydrothermal liquefaction: a technological review on reactor design and operating parameters. Bioresour Technol Rep 2023;21:101314. https://doi.org/10.1016/j.biteb.2022.101314.

[11] Haque TMA, Brdecka M, Salas VD, Jang B. Effects of temperature, reaction time, atmosphere, and catalyst on hydrothermal liquefaction of Chlorella. Can J Chem Eng 2023;101:5886–902. https://doi.org/10.1002/cjce.24839.

[12] Prestigiacomo C, Scialdone O, Galia A. Hydrothermal liquefaction of wet biomass in batch reactors: critical assessment of the role of operating parameters as a function of the nature of the feedstock. J Supercrit Fluids 2022;189. https://doi.org/10.1016/j.supflu.2022.105689.

[13] Acaru SF, Abdullah R, Lai DTC, Lim RC. Hydrothermal biomass processing for green energy transition: insights derived from principal component analysis of international patents. Heliyon 2022;8:e10738. https://doi.org/10.1016/j.heliyon.2022.e10738.

[14] Brand S, Hardi F, Kim J, Suh DJ. Effect of heating rate on biomass liquefaction: Differences between subcritical water and supercritical ethanol. Energy 2014;68:420–7. https://doi.org/10.1016/j.energy.2014.02.086.

[15] Gundupalli MP, Bhattacharyya D. Hydrothermal liquefaction of residues of *Cocos nucifera* (coir and pith) using subcritical water: process optimization and product characterization. Energy 2021;236. https://doi.org/10.1016/j.energy.2021.121466.

[16] Phuthongkhao P, Khunphonoi R, Khemthong P, Suwannaruang T, Wantala K. Bio-coal synthesis via hydrothermal carbonization of giant salvinia for a high-quality solid biofuel. Bioenergy Res 2024;17:2328–44. https://doi.org/10.1007/s12155-024-10766-z.

[17] Nagy G. The application and treatment of freshwater macrophytes as potential biogas base materials: a review. Renew Sustain Energy Rev 2024;199:114513. https://doi.org/10.1016/j.rser.2024.114513.

[18] Chanakya HN, Borgaonkar S, Meena G, Jagadish KS. Solid-phase Biogas Production with Garbage or Water Hyacinth. vol. 46. 1993.

[19] Castellanos JG, Walker M, Poggio D, Pourkashanian M, Nimmo W. Modelling an off-grid integrated renewable energy system for rural electrification in India using photovoltaics and anaerobic digestion. Renew Energy 2015;74:390–8. https://doi.org/10.1016/j.renene.2014.08.055.

[20] Kunatsa T, Madiye L, Chikuku T, Shonhiwa C. Feasibility study of biogas production from water hyacinth a case of Laka Chivero-Harare, Zimbabwe feasibility study of biogas production from water hyacinth a case of lake Chivero-Harare, Zimbabwe. Int J Eng Technol 2013;3.

[21] Ipiales RP, de la Rubia MA, Diaz E, Mohedano AF, Rodriguez JJ. Integration of Hydrothermal Carbonization and Anaerobic Digestion for Energy Recovery of Biomass Waste: An Overview. Energy & Fuels 2021;35:17032–50. https://doi.org/10.1021/acs.energyfuels.1c01681.

[22] Brown AE, Adams JMM, Grasham OR, Camargo-Valero MA, Ross AB. An Assessment of Different Integration Strategies of Hydrothermal Carbonisation and Anaerobic Digestion of Water Hyacinth. Energies (Basel) 2020;13:5983. https://doi.org/10.3390/en13225983.

[23] Chukaew P, Nakason K, Kuboon S, Kraithong W, Panyapinyopol B, Kanokkantapong V. Conversion of cassava rhizome to alternative biofuels via catalytic hydrothermal liquefaction. Asia-Pacific. J Sci Technol 2022;27. https://doi.org/10.14456/apst.2022.29.

[24] APHA. Standard Methods for the Examination of Water and Wastewater. 21st ed. Washington DC: American Public Health Association/American Water Works Association/Water Environment Federation; 2025.

[25] Ripley LE, Boyle WC, Converse JC. Improved alkalimetric monitoring for anaerobic digestion of high-strength wastes. J Water Pollut Control Fed 1986;58:406–11.

[26] Holliger C, Alves M, Andrade D, Angelidaki I, Astals S, Baier U, et al. Towards a standardization of biomethane potential tests. Water Sci Technol 2016;74:2515–22. https://doi.org/10.2166/wst.2016.336.

[27] Raposo F, De la Rubia MA, Fernández-Cegrí V, Borja R. Anaerobic digestion of solid organic substrates in batch mode: an overview relating to methane yields and experimental procedures. Renew Sustain Energy Rev 2012;16:861–77. https://doi.org/10.1016/j.rser.2011.09.008.

[28] Strömberg S, Nistor M, Liu J. Towards eliminating systematic errors caused by the experimental conditions in biochemical methane potential (BMP) tests. Waste Manage 2014;34:1939–48. https://doi.org/10.1016/j.wasman.2014.07.018.

[29] Weinrich S, Schäfer F, Liebetrau J. Value of batch tests for biogas potential analysis; method comparison and challenges of substrate and efficiency evaluation of biogas plants. IEA Bioenergy 2018.

[30] Moozhiyil M, Pallauf J. Chemical composition of the water fern, *salvinia molesta*, and its potential as feed source for ruminants. Econ Bot 1986;40:375–83. https://doi.org/10.1007/BF02858995.

[31] Tirumareddy P, Patra BR, Borugadda VB, Dalai AK. Co-hydrothermal liquefaction of waste biomass: comparison of various feedstocks and process optimization. Bioresour Technol Rep 2024;27. https://doi.org/10.1016/j.biteb.2024.101898.

[32] Wang H, Zhang M, Han X, Zeng Y, Xu CC. Production of biocrude oils from various bio-feedstocks through hydrothermal liquefaction: comparison of batch and continuous-flow operations. Biomass Bioenergy 2023;173. https://doi.org/10.1016/j.biombioe.2023.106810.

[33] Saral JS, Ranganathan P. A hydrothermal co-liquefaction of spirulina platensis with rice husk, coconut shell and HDPE for biocrude production. Bioresour Technol 2022;363. https://doi.org/10.1016/j.biortech.2022.127911.

[34] Yang C, Wang S, Ren M, Li Y, Song W. Hydrothermal liquefaction of an animal carcass for biocrude oil. Energy Fuel 2019;33:11302–9. https://doi.org/10.1021/acs.energyfuels.9b03100.

[35] Singh R, Prakash A, Balagurumurthy B, Bhaskar T. Hydrothermal Liquefaction of Biomass. Recent Advances in Thermo-Chemical Conversion of Biomass, Elsevier; 2015, p. 269–91. https://doi.org/10.1016/B978-0-444-63289-0.00010-7.

[36] De Caprariis B, De Filippis P, Petrullo A, Scarsella M. Hydrothermal liquefaction of biomass: influence of temperature and biomass composition on the bio-oil production. Fuel 2017;208:618–25. https://doi.org/10.1016/j.fuel.2017.07.054.

[37] Nakason K, Khemthong P, Kraithong W, Chukaew P, Panyapinyopol B, Kitkaew D, et al. Upgrading properties of biochar fuel derived from cassava rhizome via torrefaction: effect of sweeping gas atmospheres and its economic feasibility. Case Stud Therm Eng 2021;23:100823. https://doi.org/10.1016/j.csite.2020.100823.

[38] Cutz L, Misar S, Font B, Al-Naji M, de Jong W. Hydrothermal liquefaction of Spanish crude olive pomace for biofuel and biochar production. J Anal Appl Pyrol 2025;188. https://doi.org/10.1016/j.jaap.2025.107050.

[39] Nakason K, Kuboon S, Panyapinyopol B, Kanokkantapong V. Conversion of Cassava Rhizome to Biocrude Oil via Hydrothermal Liquefaction. 2021.

[40] Yang L, Nazari L, Yuan Z, Corscadden K, Xu C (Charles), He Q (Sophia). Hydrothermal liquefaction of spent coffee grounds in water medium for bio-oil production. Biomass Bioenergy 2016;86:191–8. https://doi.org/10.1016/j.biombioe.2016.02.005.

[41] Wang S, Wang Y, Shi Z, Sun K, Wen Y, Niedzwiecki L, et al. Van Krevelen diagrams based on machine learning visualize feedstock-product relationships in thermal conversion processes. Commun Chem 2023;6. https://doi.org/10.1038/s42004-023-01077-z.

[42] Huang Z, Wufuer A, Wang Y, Dai L. Hydrothermal liquefaction of pretreated low-lipid microalgae for the production of bio-oil with low heteroatom content. Process Biochem 2018;69:136–43. https://doi.org/10.1016/j.procbio.2018.03.018.

[43] Zhang G, Wang K, Liu Q, Han L, Zhang X. A comprehensive hydrothermal co-liquefaction of diverse biowastes for energy-dense biocrude production: synergistic and antagonistic effects. Int J Environ Res Public Health 2022;19:10499. https://doi.org/10.3390/ijerph191710499.

[44] Tian Z, Chen J, Ji X, Wang Q, Yang G, Fatehi P. Dilute sulfuric acid hydrolysis of Pennisetum (sp.) Hemicellulose. Bioresources 2017;12:2609–17. https://doi.org/10.15376/biores.12.2.2609-2617.

[45] Boeriu CG, Bravo D, Gosselink RJA, Van Dam JEG. Characterisation of structure-dependent functional properties of lignin with infrared spectroscopy. Ind Crops Prod 2004;20:205–18. https://doi.org/10.1016/j.indcrop.2004.04.022.

[46] Yang X, Lyu H, Chen K, Zhu X, Zhang S, Chen J. Selective extraction of bio-oil from hydrothermal liquefaction of *Salix psammophila* by organic solvents with different polarities through multistep extraction separation. BioResources 2014;9. https://doi.org/10.15376/biores.9.3.5219-5233.

[47] Mihajlović M, Petrović J, Kragović M, Stojanović M, Milojković J, Lopičić Z, et al. Effect of KOH activation on hydrochars surface: FT-IR analysis. Int. J. Radiat. Appl. Nat. Sci. Med. Eng. Technol. Ecol. 2017;2:65–7. https://doi.org/10.21175/radj.2017.01.014.

[48] Sun JX, Sun XF, Zhao H, Sun RC. Isolation and characterization of cellulose from sugarcane bagasse. Polym Degrad Stab 2004;84:331–9. https://doi.org/10.1016/j.polymdegradstab.2004.02.008.

[49] Ho HC, Goswami M, Chen J, Keum JK, Naskar AK. Amending the structure of renewable carbon from biorefinery waste-streams for energy storage applications. Sci Rep 2018;8. https://doi.org/10.1038/s41598-018-25880-0.

[50] Sun X, Shan R, Li X, Pan J, Liu X, Deng R, et al. Characterization of 60 types of Chinese biomass waste and resultant biochars in terms of their candidacy for soil application. GCB Bioenergy 2017;9:1423–35. https://doi.org/10.1111/gcbb.12435.

[51] Meng Y, Du H, Lu S, Liu Y, Zhang J, Li H. In situ synergistic catalysis hydrothermal liquefaction of spirulina by CuO–CeO_2 and Ni–Co to improve bio-oil production. ACS Omega 2023;8:8219–26. https://doi.org/10.1021/acsomega.2c05619.

[52] Sun Z, Liu Q, Li Y, Mazarji M, Feng L, Pan J. Deciphering the impact of lignin on anaerobic digestion: focus on inhibition mechanisms and methods for alleviating inhibition. ACS Omega 2024;9:44033–41. https://doi.org/10.1021/acsomega.4c04375.

[53] Triolo JM, Sommer SG, Møller HB, Weisbjerg MR, Jiang XY. A new algorithm to characterize biodegradability of biomass during anaerobic digestion: influence of lignin concentration on methane production potential. Bioresour Technol 2011;102:9395–402. https://doi.org/10.1016/j.biortech.2011.07.026.

[54] Gao Z, Alshehri K, Li Y, Qian H, Sapsford D, Cleall P, Harbottle M. Advances in biological techniques for sustainable lignocellulosic waste utilization in biogas production. Renewable and Sustainable Energy Reviews 2022;170:112995. https://doi.org/10.1016/j.rser.2022.112995.

[55] Sutaryo S, Sempana AN, Mulya RM, Sulistyaningrum D, Ali MS, Damarjati RI, et al. Methane production of *Pistia Stratiotes* as a single substrate and as a co-substrate with dairy cow manure. Fermentation 2022;8:736. https://doi.org/10.3390/fermentation8120736.

[56] Güngören Madenoğlu T, Jalilnejad Falizi N, Kabay N, Güneş A, Kumar R, Pek T, et al. Kinetic analysis of methane production from anaerobic digestion of water

lettuce (*Pistia stratiotes L* .) with waste sludg. J Chem Technol Biotechnol 2019;94: 1893–903. https://doi.org/10.1002/jctb.5968.

[57] O'Sullivan C, Rounsefell B, Grinham A, Clarke W, Udy J. Anaerobic digestion of harvested aquatic weeds: water hyacinth (*Eichhornia crassipes*), cabomba (Cabomba Caroliniana) and salvinia (*Salvinia molesta*). Ecol Eng 2010;36:1459–68. https://doi.org/10.1016/j.ecoleng.2010.06.027.

[58] Silivong P, Onphachanh X, Ounalom A, Preston TR. Methane production in an in vitro rumen incubation is reduced when leaves from *Mimosa pigra* are the protein source compared with *Gliricidia sepium*. Livest Res Rural Dev 2013;25.

[59] Triet T, Kiet LC, Thi NTL, Dan PQ. The invasion by Mimosa pigra of wetlands of the Mekong Delta, Vietnam. 3rd International Symposium on the Management of Mimosa pigra, Darwin, Australia; 2004, p. 29–32.

[60] Thu Hong NT, Quac VA, Kim Chung TT, Van HB, Mong NT, Huu PT. Mimosa pigra for growing goats in the Mekong Delta of Vietnam. Livest Res Rural Dev 2008;12.

[61] Rayan S, Kaewdonree S, Rangsiwiwat A, Chartchumni B. Distribution of aquatic plants in Nong Han wetland, Thailand. Songklanakarin J Sci Technol 2021;43: 195–202.

[62] Wahl CF, Diaz R, Ortiz-Zayas J. Assessing salvinia molesta impact on environmental conditions in an urban lake: case study of lago las curias. Puerto Rico Aquat Invasions 2020;15:562–77. https://doi.org/10.3391/ai.2020.15.4.02.